JOURNAL OF MATERIALS SCIENCE 22 (1987) 1799–1807

The sintering of combustion-synthesized titanium diboride

M. OUABDESSELAM, Z. A. MUNIR
Division of Materials Science and Engineering, College of Engineering, University of California, Davis, California 95616, USA

A comparative study of the sinterability of combustion-synthesized titanium diboride was conducted over the temperature range of 1800 to 2100° C. During the initial sintering stage, the densification rate was slightly higher in the combustion-synthesized than in the commercially obtained titanium diboride. For sintering times of >30 min, however, the shrinkage rates for both types of powders were the same. The activation energy for the late sintering stage was $774 \pm 46\,kJ\,mol^{-1}$, consistent with a volume diffusion mechanism, and was the same for both combustion-synthesized and commercial powders. The microstructures of sintered specimens with initial particle size below 10 μm exhibited a grain size ranging from 5 to over 40 μm after 30 min of sintering. The addition of 5 wt% NbB_2 to the combustion-synthesized resulted in enhanced shrinkage during the initial sintering stage, but did not affect later stage kinetics. Various amounts of additives of CrB_2, NiB and TiC had no effect on early and late stage sintering kinetics, with the exception of 50 wt% TiC which appreciably inhibited densification.

1. Introduction

It has often been suggested that ceramic materials formed in self-sustaining combustion reactions have enhanced sinterability [1–3]. Self-propagating high temperature synthesis (SHS), or simply combustion synthesis, involves the spontaneous formation of a compound as a combustion wave rapidly traverses a powdered mixture of the constituent elements. It is believed that due to the high exothermicity of the process, very high rates of "self-heating" and subsequent cooling of the reaction zone induce large concentrations of lattice defects in the product. Although such a picture leads to expectations of enhanced sinterability, little experimental verifications have been provided to support these expectations and at least in one case these expectations have not been verified [4]. A comparative analysis of the sintering of SHS-produced titanium diboride is presented in this paper.

The difficulty generally encountered in attempts to sinter titanium diboride (TiB_2) to high density is reflected by early investigations [5–8] conducted on powders prepared by the carbothermic method, whereby titanium dioxide is reduced in the presence of boron oxide or boron carbide. These studies suggest that the partial predominance of an evaporation–condensation mechanism at the densification temperature results in a rapid diminution of the sintering driving forces. Following an initial stage of rapid shrinkage, presumably by grain-boundary diffusion, excessive particle coarsening is reportedly induced by vapour-phase transport processes. The concomitant increase in grain size causes a reduction of grain-boundary area, which, in late sintering stages, impedes the vacancy flux needed for pore removal. In contrast to these findings, a recent study on a plasma-arc synthesized material [9] has shown that the relative ordering of critical grain growth and densification temperatures, apparently unfavourable in carbothermic TiB_2, is reversed when powders of sufficiently high purity and specific surface area are used.

The occurrence of grain growth in titanium diboride is also observed during sintering with externally applied pressure (hot-pressing). Densities near theoretical values are commonly achieved in hot-pressed compacts of the diboride, yet the mechanical properties are limited by the presence of large grains in the microstructure. The addition of various borides of the same crystal system [10], including niobium diboride (NbB_2) and chromium diboride (CrB_2), has been found to prevent grain growth during hot-pressing. The effect of these additives on grain growth during pressureless sintering, however, is not known. Furthermore, additions of nickel [11] and of tantalum carbide [12] have been found to enhance the pressureless shrinkage of carbothermic TiB_2, via liquid phase and chemical gradient effects, respectively. Additions of nickel boride (NiB), which, at the sintering temperatures, may decompose and form a liquid phase, and of titanium carbide (TiC), of the same crystal system as tantalum carbide, may, therefore, also play a role in promoting the pressureless densification of titanium diboride.

McCauley and Corbin [13] have investigated the possibility of utilizing the heat liberated in the combustion synthesis of TiB_2 to sinter the resultant product. In their study mixtures of titanium and boron powders were isostatically pressed during combustion. Although most of the product contained porosity, it was found that fully dense regions were also formed and that the porosity was the result of

0022–2461/87 $03.00 + .12

trapped impurity gases. In another study on SHS reactions under hot-pressing conditions, Zavistanos and Morris [14] obtained titanium diboride with densities of 96.6% of theoretical and microstructures typical of liquid-phase sintered materials; rounded grains below 10 μm in size.

In contrast to the high purity typically achieved in SHS ceramic materials, the properties of commercially obtained carbothermic titanium diboride are often limited by oxygen and carbon contamination. Its complete densification by pressureless sintering has not been achieved [5–8]. Plasma-arc synthesized powders of high purity and specific surface area have been experimentally prepared and successfully sintered [9]. The densification of both carbothermic and plasma-arc synthesized titanium diboride appears to occur in two steps: an initial period of rapid shrinkage which is accompanied by rapid grain growth, followed by a stage of volume diffusion-controlled densification. Shrinkage rates were used to compute the activation energies for the initial and late stages of sintering [8]. An activation energy of 309 kJ mol^{-1} was determined for the initial stage, and, in spite of markedly different shrinkage rates during that first stage, was found to be independent of initial particle size. After 30 min of isothermal holding, the activation energy for densification rose to 777 kJ mol^{-1}. The magnitude of the activation energy for the first stage is consistent with a grain-boundary diffusion mechanism. The observed increase in activation energy suggested that during the late sintering stage, shrinkage is controlled by volume diffusion.

2. The effect of additives on the sintering of titanium diboride

Enhanced densification in titanium diboride occurs under hot-pressing conditions and/or in the presence of varying amounts of additives [15]. Externally applied pressure induces stress gradients on grain boundaries, thereby promoting vacancy flow by diffusional creep, while the addition of certain metals with high solubility for the diboride, such as iron, chromium and cobalt, results in low-melting layers segregated at interparticle interfaces, in which the diffusive transport of the solid atoms is accelerated. The effect of these additives is also linked to observed decreases in lattice parameters of the diboride, brought about by the substitution of titanium atoms by the smaller additive atoms.

The identification of additives to prevent grain growth has been the focus of a recent investigation by Watanabe and Kouno [10]. These authors speculated that the presence of a solid solution between TiB_2 and metal boride of the same crystal system can enhance sintering to a high density without excessive grain growth. The TiB_2 investigated contained 1 wt % CoB as a binding agent. The addition of various borides resulted in the successful attainment of high density while grain size remained small. The effect of varying amounts of NbB_2 and CrB_2 suggests that the presence of these compounds during hot-pressing of TiB_2 resulted in an essentially complete elimination of porosity. A sensitive dependence of final porosity on NbB_2 content was observed, however, and specimens with NbB_2 content in excess of 4 wt % had substantially more porosity than those without the additive.

The effect of the presence of a liquid phase during pressureless sintering of titanium diboride was investigated by Angelini *et al.* [11]. The addition of a minimum of 5 wt % Ni promoted compact densification at temperatures around 1500° C. The resulting TiB_2 grains were rounded and an intergranular phase was present in "triple point" regions. No mention of the densification mechanism was made, however. The effect of hot-pressing in the presence of a Ni-based liquid phase was also examined, and it was found that under these conditions the samples had higher final densities and improved mechanical properties.

Shvab and Egorov [12] investigated the effect of the addition of tantalum carbide on the pressureless densification of titanium diboride. In general, shrinkage increased with the addition of TaC up to a maximum of about 25 wt % TaC, then it decreased relatively rapidly as the concentration of tantalum carbide increased.

The present work was undertaken to compare the (pressureless) sinterability of SHS-produced titanium diboride to that of commercially available powders. In addition, the effect of additives of NbB_2 and CrB_2, and of NiB and TiC, on the densification of SHS-produced titanium diboride is evaluated.

3. Experimental materials and methods

The SHS titanium diboride powder was prepared at the Lawrence Livermore National Laboratories (LLNL, Livermore, California). Powdered mixtures of titanium (obtained from Alfa Products Co.) and crystalline boron (obtained from Cerac Co.) were combusted in vacuum to form a porous TiB_2 product. The product was broken up in a boron carbide mortar and pestle, then ground in a tungsten carbide vibratory mill for 1 h. The commercial carbothermic TiB_2 powder was obtained from the Starck Company (Germany). A small quantity of SHS TiB_2 was synthesized using amorphous boron and titanium. The sintering of the resulting powder was also evaluated.

All the as-received TiB_2 powders were sieved in order to remove larger particles and thereby minimize size distribution differences between the two powders investigated. SHS and commercial powders with particle size below 10 μm were used in the sintering experiments.

Designation of the various TiB_2 powders was done according to origin and particle size distribution. The assigned acronyms are listed in Table I, and the impurity contents of the powders are shown in

TABLE I Materials designation of pure titanium diboride

Material	Particle size	Designation
SHS TiB_2	As-received	SHSAR
Commercial TiB_2	As-received	COMAR
Commercial TiB_2	Milled 48 h	COMM48
SHS TiB_2	Sieved, < 10 μm	SHS
Commercial TiB_2	Sieved, < 10 μm	COM
SHS TiB_2 (amorphous B)	Sieved, < 10 μm	SHSAB

TABLE II Impurity content in TiB_2 powders (p.p.m. by weight)

Material designation	Fe	Al	Cr	Mn	Co	W
SHSAR	< 10	< 10	45	80	< 10	40
COMAR	34	300	30	< 10	30	< 10
COMM48	1500	300	50	< 10	30	< 10
SHSAB	< 10	< 10	40	80	< 10	30

Table II. A spectrochemical evaluation of the COMAR powder was performed at LLNL and a PIXE (Proton Induced X-ray Emission) analysis of the COMM48, SHSAR, and SHSAB powders was carried out at the Crocker Nuclear Laboratory of this campus. Overall, the SHS materials were found to be of higher purity, with only manganese and tungsten being present in larger amounts in the combustion synthesized powders. Tungsten was presumably introduced in the SHS products during milling. It should be noted that substantial iron contamination appears to have occurred during milling of the commercial TiB_2.

The boride additives were purchased from Alfa Products (Danvers, Massachusetts). These included NbB_2 powder of 99.8% purity, CrB_2 powder of 99.5% purity, and NiB powder of 99.0% purity. The NiB powder, with an initial particle size of -35 mesh, was milled in ethyl alcohol for 24 h. The powder was then screened, along with the as-received CrB_2 powder, to obtain a -325 mesh ($< 44\,\mu m$) particle size. The as-received NbB_2 had a particle size below $44\,\mu m$. The titanium carbide, produced by the Starck Company, contained 300 p.p.m. (by weight) Al, and 100 p.p.m. Fe, Co, and Cr, and had a -325 mesh particle size.

As will be discussed in a later section, higher values of shrinkage were observed on specimens containing 5 wt % NbB_2. These results prompted an examination of the densification behaviour of an SHS-produced TiB_2–NbB_2 alloy. Niobium and boron powders were added to the SHS reaction mixture to produce TiB_2–NbB_2 with 5 and 10 wt % NbB_2. Designation of the powders with additives was done according to additive type and content. The compositions investigated are listed in Table III.

SEM micrographs of powders with particle size

TABLE III Materials designation for doped combustion-synthesized titanium diboride

Additive (wt %)	Designation
2% NbB_2	SHS2NB
5% NbB_2	SHS5NB
10% NbB_2	SHS10NB
15% NbB_2	SHS15NB
5% CrB_2	SHS5CB
10% CrB_2	SHS10CB
15% CrB_2	SHS15CB
5% NiB	SHS5NI
10% NiB	SHS10NI
15% NiB	SHS15NI
5% TiC	SHS5TC
10% TiC	SHS10TC
50% TiC	SHS50TC
TiB_2 + 5% NbB_2*	SHSNB5
TiB_2 + 10% NbB_2*	SHSNB10

*Samples in which boron and niobium were added before combustion-synthesis.

below $10\,\mu m$ are shown in Figs 1a and b for the combustion synthesized and commercially obtained powders, respectively. Visual examination of the powder samples at several locations indicated that the great majority of particles was approximately in the 1 to $5\,\mu m$ range in both powders.

Specific surface area measurements were made on all powders and the results of these measurements as well as the calculated equivalent spherical diameters are given in Table IV. If a spherical particle shape is assumed, the average particle size in all powders did not exceed $2.5\,\mu m$.

The various powders were formed into green compacts before being subjected to isothermal heat treatments. The powders were compacted in air using a uniaxial two-plunger stainless steel die press. Approximately 0.65 g of powder was then compacted under a pressure in the range of 2.1 to 13.8 MPa (300 to 2000 p.s.i.), resulting in a cylindrical pellet typically 0.64 cm in diameter and 0.65 cm in height, and with a density ranging from 67 to 71% of theoretical.

Sintering experiments were conducted under conditions of isothermal heating, for sintering times of 30, 60, and 120 min. Four sintering temperatures were selected, ranging from 1800 to 2100° C, in 100° C

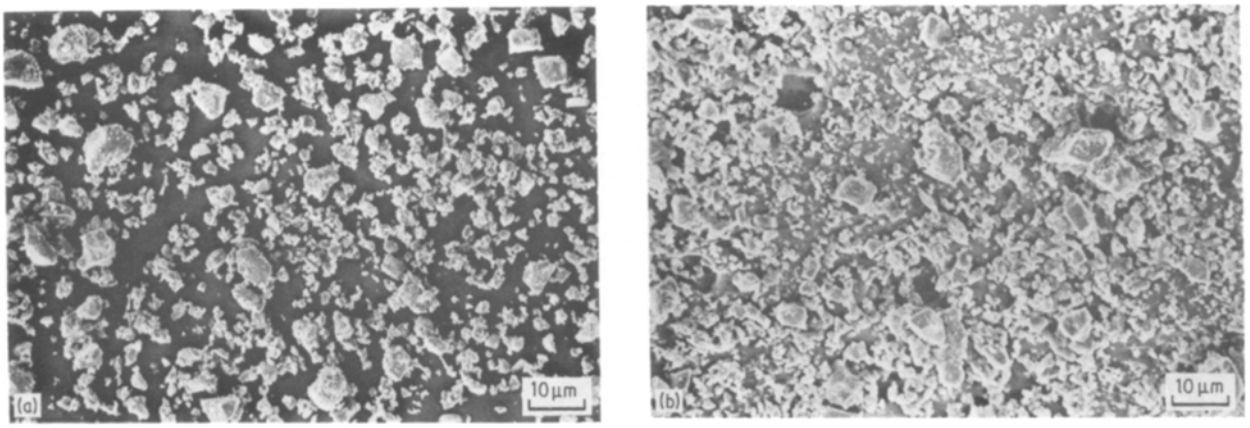

Figure 1 (a) SEM micrograph of sieved ($< 10\,\mu m$) combustion-synthesized TiB_2. (b) SEM micrograph of sieved ($< 10\,\mu m$) commercially available TiB_2.

TABLE IV Specific surface area of TiB_2 powders

Material	Specific surface area ($m^2 g^{-1}$)	Equivalent spherical diameter (μm)
SHSAR	0.60	2.22
COMAR	0.60	2.22
COMM48	1.21	1.10
SHS	1.29	1.03
COM	1.17	1.14
SHSAB	1.32	1.01

TABLE V Maximum linear shrinkage of sieved TiB_2 compacts after 2 h at sintering temperature

Temperature (° C)	Shrinkage (%)	
	SHS	COM
1800	10.1	9.7
1900	11.9	11.4
2000	14.0	13.1
2100	15.5	14.6

intervals. Temperatures were measured to an accuracy of $\pm 10°$ C with an optical pyrometer. High vacuum (10^{-5} torr) was used as the sintering atmosphere.

Sintering time was counted from the moment that the sample had reached the sintering temperature. As a result, shrinkage and related results for the higher temperature runs were affected by sintering at lower temperatures during heat-up.

4. Results and discussion

4.1. Comparative sinterability of undoped TiB_2

The sinterability of the SHS titanium diboride was compared to that of the commercial TiB_2 by examining variations in linear shrinkage for both powders. Specimen weight loss during sintering was determined by weighing the samples before and after the heat treatment. The results indicated that generally weight loss occurred during the first 30 min of isothermal heating. Weight loss was approximately 4% at 1800° C and 6% at 2100° C, and did not vary with sintering time. Weight reduction during the initial sintering stage is significantly lower (by about 50%) than that reported in an earlier investigation [7]. Results of the sintering experiments conducted on powders with a maximum particle size of 10 μm are shown in Figs 2 and 3 for the SHS and COM powders, respectively. The maximum linear shrinkages after 2 h at the sintering temperatures are shown in Table V.

Using amorphous boron as an initial reactant in the SHS preparation of titanium diboride apparently had no effect on the sintering behaviour of the resulting powder. Fig. 4 shows that the shrinkage data at 1900 and 2100° C were identical for SHS and SHSAB powders, suggesting that SHS titanium diboride prepared with amorphous boron was as sinterable as that prepared with crystalline boron.

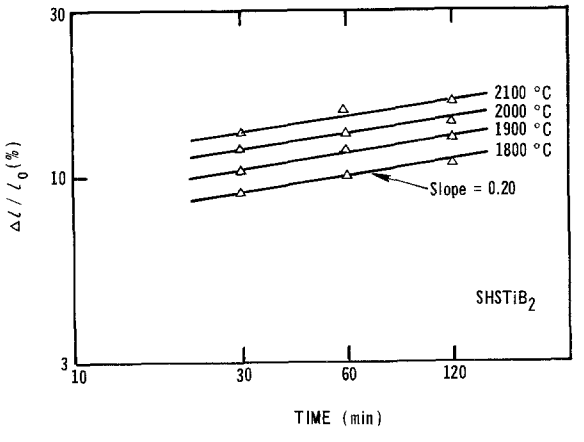

Figure 2 The variation of shrinkage with time for SHS TiB_2 powder.

Porosities in sintered samples were determined from the shrinkage and weight loss measurements. The kinetics of porosity removal for SHS and COM powders are shown in Fig. 5 for sintering at 1900 and 2100° C. It can be seen from these variations that with an increase in sintering time, porosity in SHS specimens remained lower than in commercial specimens, and that the rate of porosity reduction for specimens pressed from both powders was greatly diminished after the initial 30 min of sintering. At the higher temperature, differences between the two powders were not as pronounced. The variations of porosity with time are representative of the shrinkage behaviour during isothermal holding.

The results obtained from the linear shrinkage measurements suggest that the densification mechanism in the time interval which followed the initial 30 min of sintering was the same in both SHS and COM powders, and did not change with temperature. The activation energy for densification in this late sintering stage was determined from a plot of the log of shrinkage against the inverse of the absolute temperature of sintering at $t = 120$ min, Fig. 6. Using the kinetic exponent n obtained from the log $\Delta l/l_0$ against log t plots, an activation energy of 744 ± 46 kJ mol^{-1} was calculated. This is in fair agreement with the results of Kislyi *et al.* [8], who found a late stage activation energy of 777 ± 50 kJ mol^{-1}, and suggested that volume diffusion is the operative densification mechanism during the late sintering stage of titanium diboride.

Grain and pore structures observed on sintered SHS specimens were similar in character to those exhibited by compacts pressed from the commercial powder. In general, nonuniform grain growth resulted

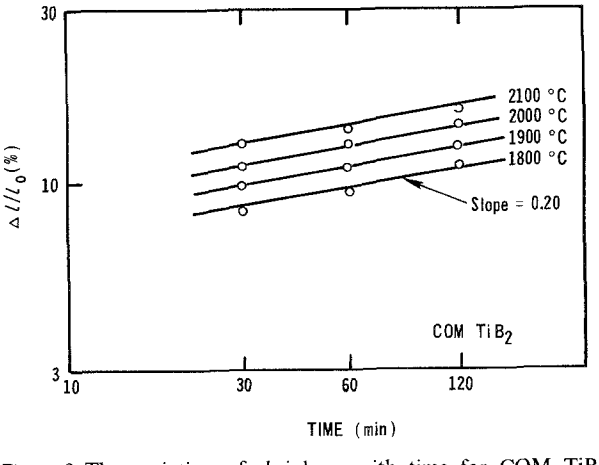

Figure 3 The variation of shrinkage with time for COM TiB_2 powder.

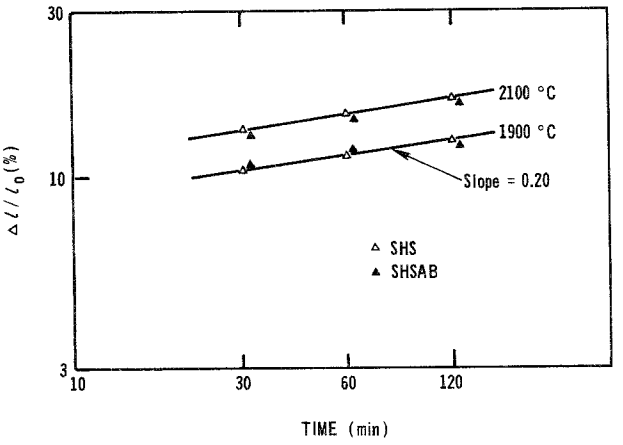

Figure 4 Shrinkage of combustion-synthesized titanium diboride made from crystalline (SHS) and amporphous (SHSAB) boron powders.

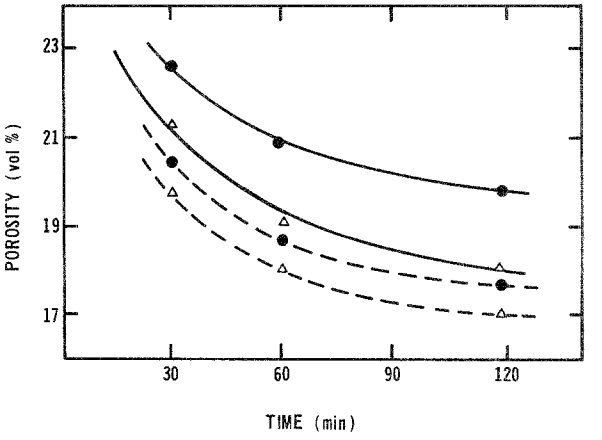

Figure 5 The variation of porosity with time for commercially obtained (COM) and combustion-synthesized (SHS) TiB_2 powders sintered at 1900° C. (●) COM, (△) SHS, (——) 1900° C, (– – –) 2100° C.

in a wide range of grain sizes in sintered TiB_2. The microstructures in Figs 7a and b correspond to specimens of both origins sintered for 2 h at 2100° C. Fewer large pores in compacts sintered at this temperature allowed the etching of relatively large solid regions, revealing the presence of grains ranging in size from below 5 μm to approximately 40 μm. While some elongated shapes were found, most grains had square or polygonal cross-sections. The thick appearance of some grain boundaries on these micrographs is probably due to overextended etching times.

The effect of temperature on pore and grain size is illustrated in Figs. 8a and b. At lower temperatures (Fig 8a), microstructures of sintered specimens were characterized by large amounts of porosity, and by interconnected solid regions separated by large pores. At higher temperatures (Fig. 8b), grain size was larger and less uniform, and noticeably less porosity was present. It should be noted that porous regions as large as those shown in Fig. 8a were also found on specimens sintered at the higher temperatures, although at a much lower frequency of occurrence. Relatively dense regions such as the one shown in Fig. 8b were characteristic of specimens sintered at 2000 and 2100° C.

Changes in microstructure with sintering time during late stage densification are illustrated in Figs 9a and b. Grain size and porosity were only slightly affected by sintering time, suggesting that the significant microstructure developments occurred during the initial stage of sintering. Large grains were already present in the microstructure after 30 min, and became slightly larger with time. Smaller grains appeared stable during the late sintering stage.

These observations were common to specimens prepared from both SHS and commercial powders. The rapid grain growth reported to occur between 200 and 2100° C [5, 9], was not observed in this study. With the exception of the very large grains already present after 30 min of sintering, and which appeared to grow with sintering temperature, grain size was independent of sintering time during the late sintering stage, suggesting that the average rate of grain growth had sharply dropped by the end of the initial sintering period.

Pores in sintered titanium diboride were mostly rounded in shape, with some being highly irregular in shape. An average size of approximately 10 μm was typical of microstructures sintered above 1900° C. Pores appreciably larger than unsintered interparticle

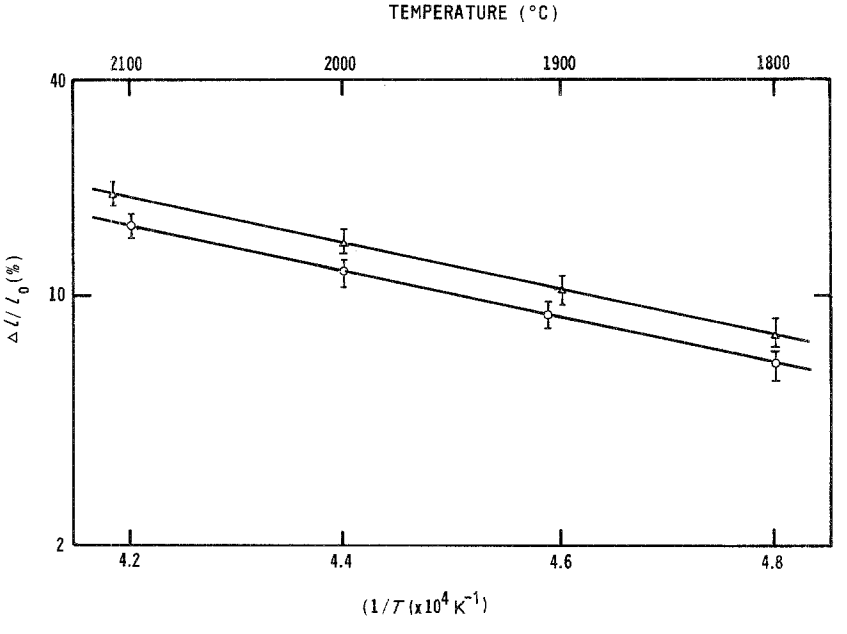

Figure 6 The temperature dependence of shrinkage for COM and SHS TiB_2 compacts sintered for 120 min. (○) COM, (△) SHS.

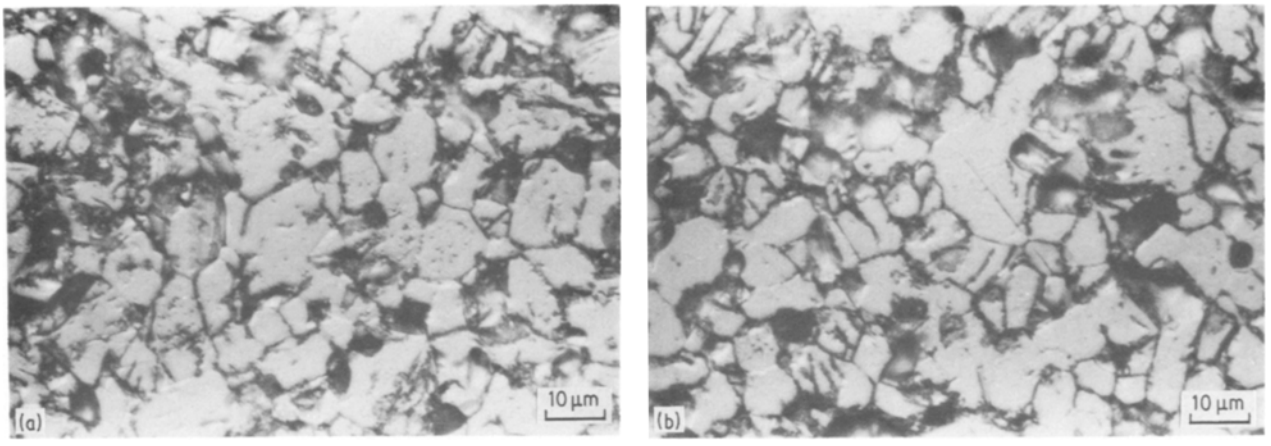

Figure 7 (a) Micrograph of SHS TiB_2 sintered at 2100° C for 120 min. (b) Micrograph of COM TiB_2 sintered at 2100° C for 120 min.

voids were found in specimens sintered at all temperatures, but were mostly found in specimens sintered at 1800 and 1900° C.

Similarities in sintered microstructures between SHS and commercial powder compacts could also be visualized on fracture surface SEM micrographs. In Figs 10a and b, specimens of both origins sintered at 1800° C for 1 h are shown. Particle coarsening appears to have occurred in these specimens, presumably by an evaporation–condensation mechanism during the initial 30 min of sintering. Agglomeration of smaller particles can also be seen, along with some interparticle necking.

The morphology of the pore surfaces at higher temperatures is shown in Figs 11a and b, on sintered as-received TiB_2 specimens. After 1 h at 1900° C (Fig. 11a), smaller particles had coalesced into dense clusters surrounded by coarse particles and by numerous small voids. Crystal growth patterns can also be seen on the larger particles, which had probably undergone coarsening via a vapour-phase process. The general appearance of the larger regions of interconnected fine particles is also characteristic of specimens pressed from seived powders sintered at 1900° C. Virtually no large particles were found in those specimens. After 1 h at 2100° C (Fig. 11b), smaller particles could no longer be identified, as particle coarsening and coalescence into dense regions occurred to a larger extent than at 1900° C. Interparticle neck growth is readily seen, however, along with striations, and pore surfaces are smooth and rounded. The particle in the centre of the micrograph appears to have fractured along three necks.

4.2. The influence of boride and carbide additives on the sintering of TiB_2

Experiments aimed at determining the effect of the various boride and carbide additives on the kinetics of shrinkage of SHS titanium diboride were conducted on sieved powders ($< 10\,\mu m$). The results of the experiments on NbB_2 addition are presented in Fig. 12 for temperatures of 1900 and 2100° C. It appears that specimens containing 5 wt % NbB_2 had reached a higher shrinkage at the end of the first 30 min of sintering, suggesting that the rate of shrinkage during the initial period may have been higher in specimens containing that amount of additive. On the other hand, concentrations of 10 and 15 wt % NbB_2 had no effect on the sintering behaviour of SHS TiB_2. Shrinkage attained after the initial 30 min of sintering by specimens containing these amounts was approximately equal to that reached by undoped SHS specimens sintered at the corresponding temperatures. Furthermore, the kinetic exponent n (the slope of log $\Delta l/l_0$ against t plots) was not affected by the additive content at all concentrations of NbB_2 investigated. The effect of a smaller NbB_2 content on the kinetics of sintering was later examined. An amount of 2 wt %

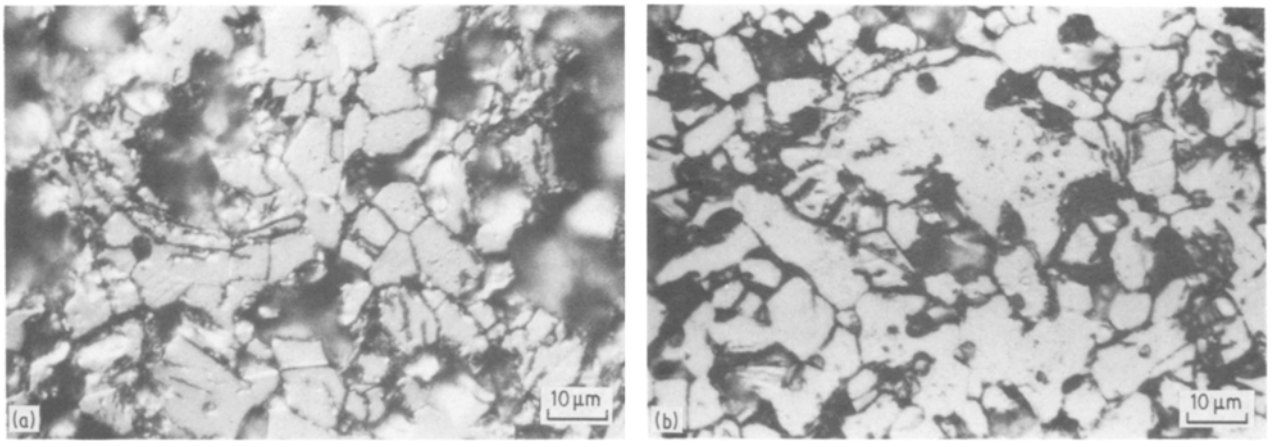

Figure 8 (a) Micrograph of SHS TiB_2 sintered at 1900° C for 120 min. (b) Micrograph of SHS TiB_2 sintered at 2100° C for 120 min.

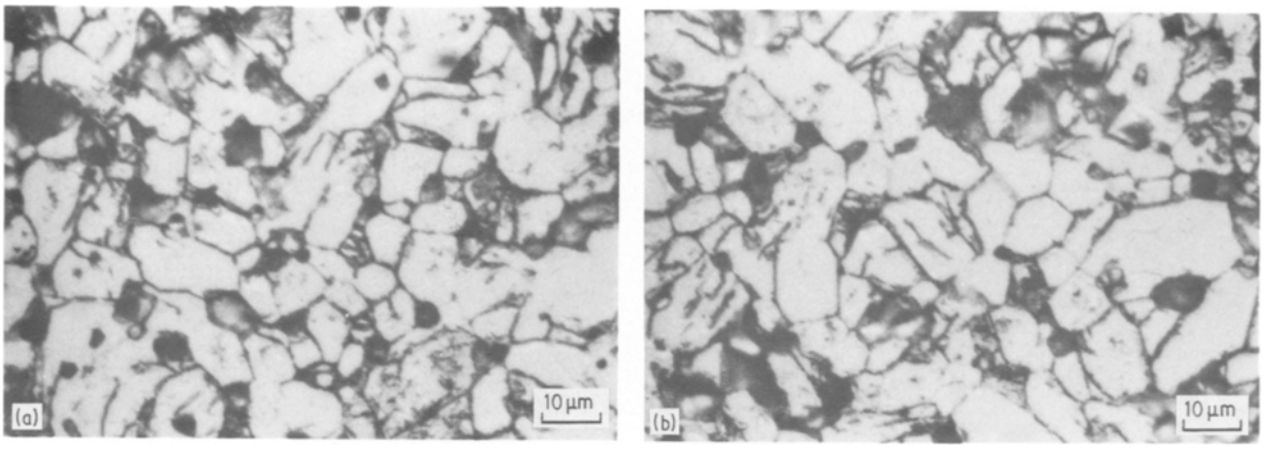

Figure 9 (a) Micrograph of SHS TiB_2 sintered at 2100° C for 30 min. (b) Micrograph of SHS TiB_2 sintered at 2100° C for 120 min.

NbB_2 was added to the SHS powder and sintered in a crucible containing undoped SHS specimens. As can be seen in Fig. 12, this amount did not affect densification, and the maximum shrinkage for the samples containing 2 wt % NbB_2 (SHS2NB) after 30 min of sintering was approximately equal to that of undoped specimens.

Additions of CrB_2 (5 to 15 wt %) did not affect the kinetics of pressureless sintering of SHS TiB_2. Likewise, the addition of NiB to SHS titanium diboride resulted in unaltered shrinkage kinetics relative to the undoped sample.

The results of adding TiC as a dopant to TiB_2 are shown in Fig. 13. The curves in Fig. 13 indicate that final stage sintering kinetics were again unaffected by additions of 5 and 10 wt % TiC, and that an amount of 10 wt % TiC resulted in a slight, and probably insignificant drop in initial shrinkage rate. However, a marked effect was observed on specimens prepared with 50 wt % TiC. Shrinkage in these samples was noticeably slower in the initial stage, as evidenced by a maximum shrinkage of 6.5% after 30 min at 2000° C, compared to approximately 14% for most of the other powders investigated. The shrinkage rate in the late sintering stage was also appreciably reduced: the kinetic exponent, n, was measured at 0.11 as compared to 0.2 for the undoped TiB_2 or for TiB_2 doped with lower concentrations of TiC.

Specimens pressed from SHS titanium diboride prepared by including niobium and boron powders in the combustion mixture to obtain concentrations of 5 and 10 wt % NbB_2 were subjected to a series of sintering experiments in order to evaluate their relative sinterability. Based on the results obtained on the SHS5NB powders, i.e. those to which 5 wt % NbB_2 was added after combustion, an enhancement of initial stage densification kinetics was expected. The results depicted in Fig. 14, however, show the sintering behaviour of these powders to be very similar to that of pure SHS TiB_2 powder. Boron may have partially evaporated during the combustion process such that a lower amount of NbB_2 may have formed, and as shown earlier (Fig. 12) the addition of 2 wt % NbB_2 had no effect on the shrinkage of TiB_2.

The shrinkage behaviour of the SHS specimens after the first 30 min of sintering was nearly identical to that of compacts pressed from the commercial powders. At all temperatures investigated, the shrinkage rate fell to a very low value and remained constant with extended sintering time. This, as indicated earlier is in agreement with previously reported late sintering stage features in titanium diboride [5–9]. No evidence of an enhanced sintering activity in the SHS powders, presumably because of the presence of high concentrations of lattice defects was therefore found. This could be explained by the fact during heat-up and early sintering stages, recovery within the powder particles may have occurred leading to the relief of residual

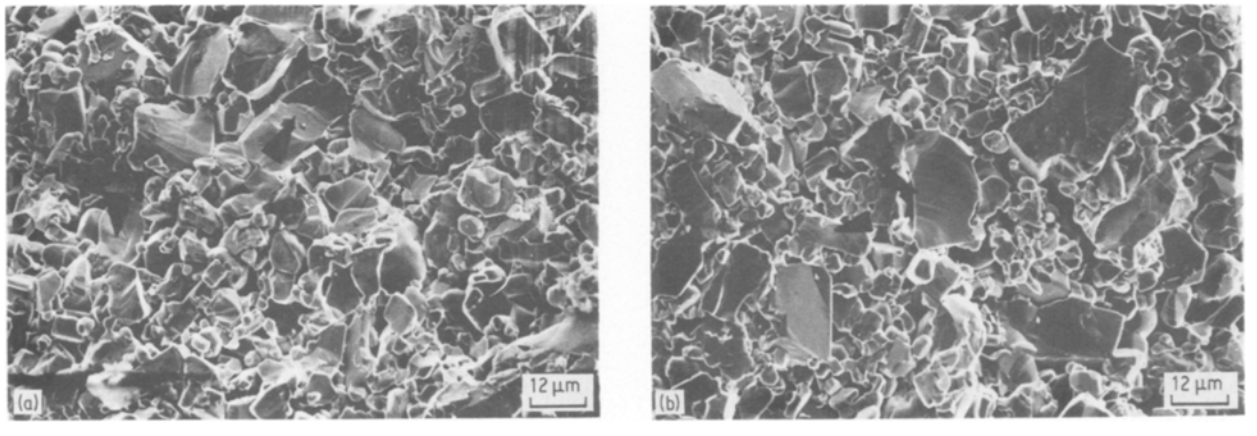

Figure 10 (a) SEM fracture surface of SHS TiB_2 sintered at 1800° C for 60 min. (b) SEM fracture surface of COM TiB_2 sintered at 1800° C for 60 min.

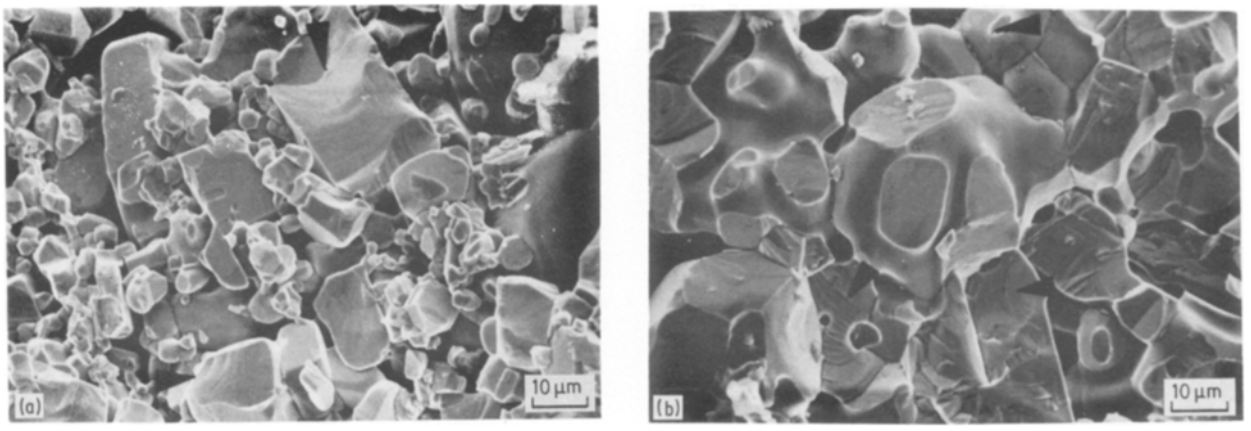

Figure 11 (a) SEM fracture surface of SHS TiB_2 (as-received) sintered at 1900° C for 60 min. (b) SEM fracture surface of SHS TiB_2 (as-received) sintered at 2100° C for 60 min.

stresses, thereby eliminating the potential sinterability of defect-containing materials. It should be noted that regardless of lattice defect concentration, grain size during late stage densification of covalently bonded substances (such as TiB_2) should imperatively be small to provide the required boundary area for vacancy flux [9, 16]. This could only result from inhibited grain growth during the early stage of sintering, an occurrence which is presumably independent of defect concentration.

5. Conclusions

Small differences in shrinkage rate between SHS and commercial titanium diboride were found in the early stage of sintering ($t < 30$ min). For equivalent initial conditions of particle size distribution and specific surface area, the SHS specimens had reached approximately 8% more linear shrinkage at the end of the first 30 min of sintering, suggesting that the SHS titanium diboride had a higher sintering activity during the initial sintering stage. The kinetics of densification during the late sintering stage of SHS titanium diboride were identical in character to those measured on commercial powders. These comparative results appeared to be independent of temperature in the range investigated.

The activation energy for the late sintering stage was 744 ± 46 kJ mol^{-1}, and was the same for both SHS and commercial powders over the temperature range investigated. This activation energy is consistent with a densification process controlled by volume diffusion, and is in agreement with a previously reported value [7].

No differences between SHS and commercial titanium diboride were observed in the sintered microstructures. Discontinuous grain growth was observed at temperatures of 1900° C and above in specimens pressed from both powders, and appeared to have

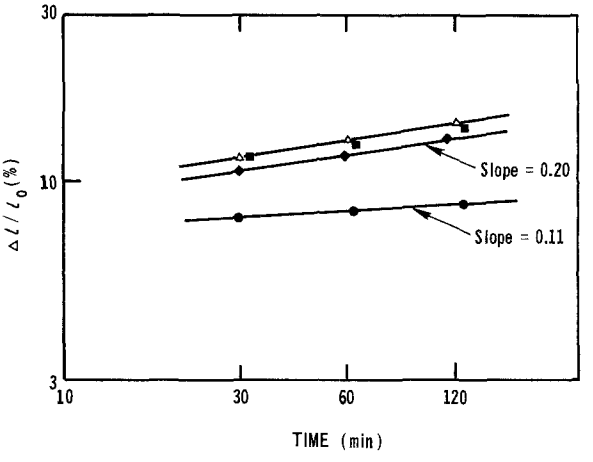

Figure 13 Effect of addition of TiC on the sintering of SHS TiB_2. (△) SHS, (■) SHS5TC, (◆) SHS10TC, (●) SHS50TC. T = 2000° C.

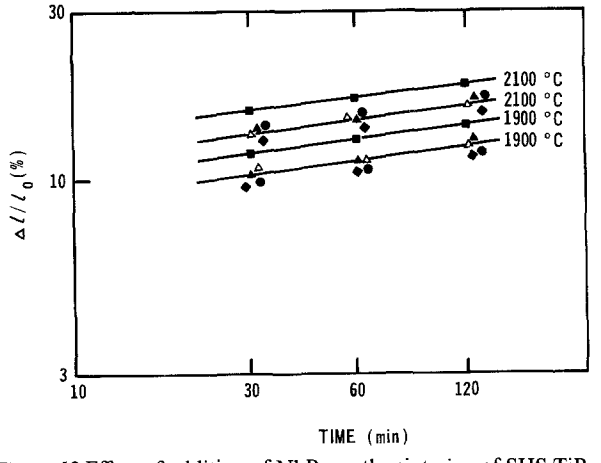

Figure 12 Effect of addition of NbB_2 on the sintering of SHS TiB_2. (△) SHS, (▲) SHS2NB, (■) SHS5NB, (◆) SHS10NB, (●) SHS15NB.

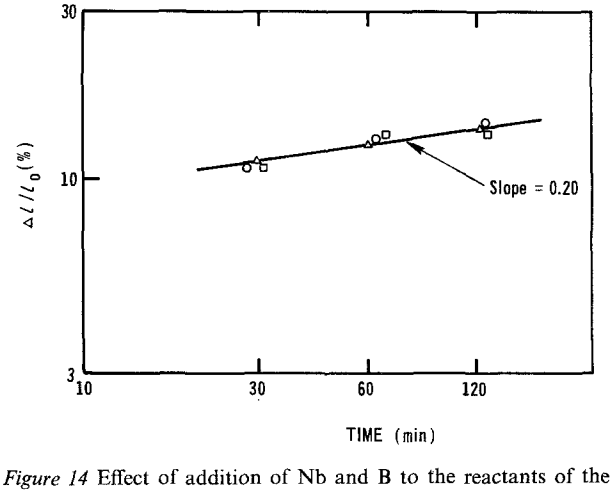

Figure 14 Effect of addition of Nb and B to the reactants of the combustion synthesis of TiB_2. (△) SHS, (○) SHSNB5, (□) SHSNB10. T = 2000° C.

occurred primarily during the initial stage. Large pores were found in all analysed specimens; their presence was noted mainly in specimens sintered at lower temperatures.

A content of 5 wt % niobium diboride increased the shrinkage rate of SHS titanium diboride during the initial sintering stage. Late stage densification, however was not affected by the presence of the additive. Amounts of 5, 10 and 15 wt % CrB_2 and NiB, and of 5 and 10 wt % TiC had no effect on the densification behaviour of SHS titanium diboride, while the addition of 50 wt % TiC caused a sharp drop (of approximately 50%) in overall shrinkage kinetics.

Acknowledgements

The combustion-synthesis of titanium diboride was performed at the Lawrence Livermore National Laboratory (LLNL). We are grateful to Dr J. B. Holt and his colleagues, D. Kingman and G. Bianchini, for providing the samples.

References

1. A. G. MERZHANOV, G. G. KARYNK and I. P. BOROVINSKAYA, *Soviet Powder Met.* **20** (1981) 209.
2. A. G. MERZHANOV and I. P. BOROVINSKAYA, *Acad. Sci. USSR Chem. Phys.* **204** (1972) 366.
3. O. R. BERGMANN and J. BARRINGTON, *J. Amer Ceram. Soc.* **49** (1966) 502.
4. B. MANLEY, J. B. HOLT and Z. A. MUNIR, in "Sintering and Heterogeneous Catalysis, Materials Science Research", Vol. 16, edited by G. C. Kuczynski, A. E. Miller and G. A. Sargent (Plenum Press, New York, 1984) p. 303.
5. G. V. SAMSONOV and M. S. KOVAL'CHENKO, *Poroshk. Met.* **1** (1961) 2029. (English Translation: AEC-tr-5604. Washington, DC.)
6. R. L. COBLE and H. A. HOBBS, in "Investigation of Boride Compounds for Very High Temperature Applications", edited by L. Kaufmann and R. L. Clougherty, N.T.I.S., (Springfield, Virginia, 1963).
7. P. S. KISLYI and O. V. ZAVERUKHA, *Soviet Powder Met.* **7** (1970) 549.
8. P. S. KISLYI, M. A. KUZENKOVA and O. V. ZAVERUKHA, *Phys. Sintering* **4** (1972) 107.
9. H. R. BAUMGARTNER and R. A. STEIGER, *J. Amer. Ceram. Soc.* **66** (1983) 207.
10. T. WATANABE and S. KOUNO, *Bull. Amer. Ceram. Soc.* **61** (1982) 970.
11. P. ANGELINI, P. F. BECHER, J. BENTLEY, C. R. FINCH and P. S. SKLAD, *Mat. Res. Soc. Symp. Proc.* **24** (1984) 299.
12. S. A. SHVAB and F. F. EGOROV, *Sov. Powder Met.* **22** (1983) 261.
13. J. W. McCAULEY, N. D. CORBIN, T. RESETAR and P. WONG, *Ceram. Eng. Sci. Proc.* **3** (1982) 538.
14. P. D. ZAVISTANOS and J. R. MORRIS Jr, *Ceram. Eng. Sci. Proc.* **4** (1983) 624.
15. H. PASTOR, in "Boron and Refractory Borides," edited by V. I. Malkovich, (Springer-Verlag, New York, 1977) p. 457.
16. C. GRESKOVICH and J. H. ROSOLOWSKI, *J. Amer. Ceram. Soc.* **59** (1976) 336.

Received 4 July
and accepted 9 September 1986